05,01

Dzyaloshinskii–Moriya interaction in Pt/Co/Ir/Co/Pt synthetic ferrimagnets

© A.I. Bezverkhnii[1], V.A. Gubanov[2], A.V. Sadovnikov[2], R.B. Morgunov[1,¶]

[1] Institute of Problems of Chemical Physics, Russian Academy of Sciences, Chernogolovka, Russia
[2] Saratov State University, Saratov, Russia

¶ E-mail: morgunov2005@yandex.ru

Received May 19, 2021
Revised August 2, 2021
Accepted August 3, 2021

We had found nonreciprocity of spin waves in Pt/Co/Ir/Co/Pt synthetic ferrimagnets by Brillouin light scattering technique. It is shown that the main contribution to the nonreciprocity of spin waves is made by the Dzyaloshinskii–Moriya interaction with an energy density $D \approx 1.7-2.3$ erg/cm^2. The energy density of the Dzyaloshinsky–Moriya interaction in Pt/Co/Ir/Co/Pt synthetic ferrimagnets is higher than its values in heterostructures with one Co layer Pt/Co(1 nm)/Ir ~ 1.4 erg/cm^2. The D value of synthetic ferrimagnets decreases with increasing thickness of the Co thin layer.

Keywords: synthetic ferrimagnets, perpendicular magnetic anisotropy, Brillouin light scattering, exchange interaction, Dzyaloshinskii–Moriya interaction .

DOI: 10.21883/PSS.2022.14.54330.120

1. Introduction

Multilayered heterostructures and superlattices are of interest in the field of studying spin waves (SW), since they are the basis for antiferromagnetic spintronic devices [1]. In the first works devoted to the study of SW by the method of Mandelstam-Brillouin spectroscopy (MBS) in spintonic structures [2,3], the objects of study were heterostructures consisting of two ferromagnetic layers with easy magnetization axes in the plane, separated by a layer of non-magnetic conductive material (FM/NM/FM). The MBS method is a spectroscopy of elastic scattering of light by natural vibrations of a solid body with a change in the frequency of the scattered photon. Scattering can occur both on phonons and on spin waves (magnons). The maxima in the MBS spectra correspond to the frequencies of phonons and spin waves at which the photon was scattered.

The MBS frequency spectra of single thin ferromagnetic films exhibit two scattering peaks on spin waves: a Stokes peak and an anti-Stokes peak [4]. These peaks correspond to SW propagating in thin films in directions opposite to each other and orthogonal to the direction of the effective magnetic field. In FM/NM/FM multilayer heterostructures consisting of two exchange-coupled ferromagnetic layers, the MBS spectra can differ from the spectra of single ferromagnetic films by the presence of two Stokes peaks and two anti-Stokes peaks [3], which is a manifestation of SW dispersions in exchange-coupled ferromagnetic layers. When the thickness of the interlayer between the layers of the ferromagnet changes, the energy J_{12} of the interlayer exchange interaction Ruderman–Kittel–Kasuya–Yosida (RKKY) changes. In the Fe/Au/Fe and Fe/Cr/Fe samples [3], a change in the frequency of one Stokes peak and one anti-Stokes peak of spin waves was found with a change in J_{12}. The frequencies of the remaining peaks did not depend on J_{12}. The exchange interaction between spins separated by an interlayer of ferromagnetic layers leads to the coordinated propagation of spin waves in them, which can be represented as a superposition of the acoustic and optical branches of the spectrum. The frequencies of spin waves, which do not depend on J_{12}, belong to the acoustic mode. The acoustic mode is associated with coupled in-phase spin waves with the same values k in two ferromagnetic layers (Fig. 1). The optical mode is caused by the interlayer antiferromagnetic exchange interaction between spins in ferromagnetic layers. As a result of the antiferromagnetic exchange between the spins, they gyrates in antiphase [2,5].

Another consequence of the interaction between ferromagnetic layers is the difference Δf between the frequencies of the Stokes peak $f(k)$ and the anti-Stokes peak $f(-k)$. This frequency difference depends on the surface anisotropy of two ferromagnetic layers [6], on the dipole interaction, and on the energy of the Dzyaloshinskii–Moriya antisymmetric exchange interaction (DMI) [7], which appears at the interfaces between the ferromagnet and heavy metal with strong spin-orbit interaction [8]. In the literature, the difference between the frequencies of the Stokes and anti-Stokes Δf peaks (nonreciprocity of spin waves) is often mistakenly perceived as unambiguous evidence of the presence of DMI and is used to measure the energy density of DMI — D. Although the MBS method is a powerful tool for the direct measurement of DMI energy, other sources of Stokes and anti-Stokes peak frequency nonreciprocity should be taken into account to use it.

Most of the work on measuring the DMI energy density by the MBS method has been done in heterostructures based on single ferromagnetic films, but it is of interest to complicate this situation in FM/NM/FM structures due to the exchange bias, interlayer exchange RKKY, and the difference in the surface anisotropy constants of two ferromagnetic layers. For example, in [9] accurate measurements of MBS were carried out in Co/Au/Co and Co/Cu/Co samples, in which the Co thicknesses were the same, and the thickness of the interlayer inside one sample varied stepwise with a step of 0.4 nm. Thus, the authors [9] were able to correctly take into account the influence of surface and magnetocrystalline anisotropy on the spectrum of spin waves in Co layers. This allowed to accurately measure the interlayer exchange energy J_{12} by the MBS method as a function of only the thickness of the Au and Cu interlayers, excluding the contribution of surface anisotropy. As a result, a sign-alternating oscillation of the energy of the interlayer exchange interaction was discovered with a change in the thickness of the interlayer. Later, by the same method, the oscillation of the exchange interlayer energy in $[Co/Ru]_{20}$ superlattices was discovered [10].

It is known from the literature that there is DMI with energy density $D \sim 1\,erg/cm^2$ at the Pt/Co and Pt/Ir interfaces in the Pt/Co/Pt [11,12], Pt/Co/Ir/Pt [13] and Pt/Co/Ir [14] heterostructures. In the Pt/Co/Ir/Co/Pt samples studied by us, the presence of DMI can also be expected, since the samples contain Pt/Co and Pt/Ir interfaces. In the literature, studies of DMI in heterostructures based on a single Co film [11–14] are widely represented, while DMI in exchange-coupled ferromagnetic layers is poorly studied. The purpose of this paper is to study the spin dynamics by the MBS method in synthetic ferrimagnets (SF) Pt/Co/Ir/Co/Pt, in which the antiferromagnetic exchange interaction between the Co layers and DMI at the Pt/Co and Pt/Ir interfaces is combined.

2. Samples and experimental procedure

The samples under study are multilayer heterostructures SiO2/Pt(3.2 nm)/Co(1.1 nm)/Ir(1.4 nm)/Co(t_{Co})/Pt(3.2 nm), where t_{Co} — the thickness of the upper Co layer is 0.6, 0.7, 0.8 and 1.0 nm. Samples 2×3 mm in size were obtained by magnetron sputtering at room temperature in ultrahigh vacuum (10^{-8} Torr). Co layers have perpendicular magnetic anisotropy due to the hybridization of Co atomic 5*d*-orbitals with Pt and Ir orbitals [15]. Detailed studies of the magnetic properties and magnetization reversal dynamics of these samples were presented in the works [16,17], where the layer anisotropy energies, exchange interactions between layers, critical fields of magnetization switching, and other properties were established.

The magnetic hysteresis loops at orientations of the external magnetic field along the sample surface (H_{IP}) and perpendicular to it (H_{OP}) were recorded by a Quantum Design MPMS 5XL SQUID magnetometer.

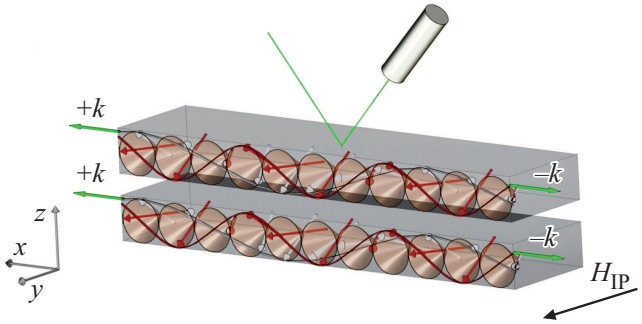

Figure 1. Spin waves in a synthetic antiferromagnet in a constant external magnetic field H_{IP}.

To measure the light scattering spectra by the MBS method at room temperature, the Damon–Eshbach geometry and the backscattering configuration were used, i.e. the external field H_{IP} was directed in the film plane perpendicular to the SW wave vector and perpendicular to the light incidence plane (see Fig. 1). The measurements were carried out at angles of incidence of the laser beam of 15, 30, 45, and 60°. These angles correspond to the projections of the wave vector of light incident on the surface of the sample, equal to $k_{x1} = 7\,\mu m^{-1}$, $k_{x2} = 11\,\mu m^{-1}$, $k_{x3} = 16\,\mu m^{-1}$ and $k_{x4} = 20\,\mu m^{-1}$. The light source was a laser beam with a wavelength of 532 nm, generated by a single-frequency Excelsior laser (Spectra Physics) EXLSR-532-200-CDRH. The diameter of the laser spot focused on the sample surface was 25 μm. The laser radiation power 20 mW was low enough not to lead to heating of the sample. It is important to note that the effective penetration depth of the laser beam is 30−40 nm [18], which exceeds the total thickness of the layers of the studied heterostructures. Thus, all data obtained by the MBS method are caused by the total contribution of all layers. The frequency differences between the Stokes and anti-Stokes peaks were determined from measurements carried out in an external constant magnetic field with a strength of +8 kOe. This external field is close to the effective anisotropy field determined from Fig. 2. The magnitude of this field was sufficient to orient the spins in the plane of the sample. The recording of MBS spectra is a process of long-term signal accumulation. The accumulation time on the samples studied in this article was 10−12 h. During this time, an average of 100 measurements were made for each frequency in the range from −30 GHz to +30 GHz with a step of 125 MHz.

Mathematical modeling of spin wave dispersion $f(k_x)$ and dependence of spin wave frequency on interlayer exchange energy $f(J_{12})$ was carried out using Wolfram Mathematica 12.1 software.

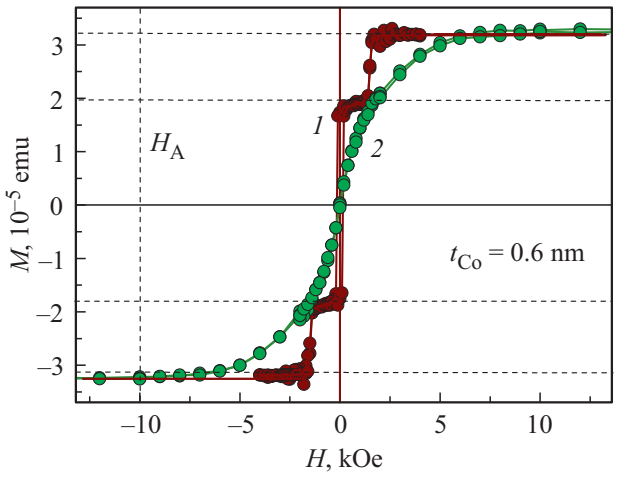

Figure 2. Field dependences of the magnetization M(H) of the sample with $t_{Co} = 0.6$ nm, recorded with the field directed perpendicularly (*1*) and parallel (*2*) plane of the sample. The dashed horizontal lines show the equilibrium states of the sample magnetization in a field directed normally to the sample surface. The vertical dashed line shows the effective magnetic anisotropy $H_A = 10$ kOe.

3. Results and discussion

In the MBS spectra of samples with $t_{Co} = 0.7$, 0.8 and 1.0 nm there was one Stokes peak and one anti-Stokes peak each (Figs 3, *a*–3, *c*). In the spectrum of the sample with $t_{Co} = 0.6$ nm (Fig. 3, *d*) there were two Stokes peaks and two anti-Stokes peaks. There were similar double spectra in [2,3,6,7]. Two peaks, the frequencies of which do not depend on the interlayer exchange energy, belong to the SW acoustic mode. Spin waves the frequencies of which depend on the interlayer exchange belong to the optical mode. By the ratio of the intensity of the Stokes and anti-Stokes peaks, it was a guide to the ratio between the number of events of photon scattering on SW with vectors $+k_x$ (Stokes) and (anti-Stokes) $-k_x$. The number of SW scattering events depends on the lifetime of the corresponding magnons [19]. The intensity ratio of the Stokes and anti-Stokes peaks (see Fig. 3) for all samples was approximately the same $I_S/I_{AS} \sim 1.18$. Consequently, the ratio of the average lifetime of magnons with $+k_x$ to the average lifetime of magnons with the opposite wave vector k_x was the same in all samples.

To verify that the presence of two Stokes peaks and two anti-Stokes peaks in the MBS spectrum of the sample with $t_{Co} = 0.6$ nm is caused by the optical and acoustic modes, the frequency dependence of the spin waves f on the value of the exchange interlayer energy J_{12} was modeled in accordance with the model proposed in [20]. In contrast to the model presented in [21] for single-layer structures, calculations are proposed in [20] to describe synthetic antiferromagnetics and ferrimagnets with perpendicular magnetic anisotropy. The following parameters were chosen for modeling: the same field of cubic anisotropy of the lower and upper Co layers $H_{ac1} = H_{ac2} \approx 152$ Oe [22], equal field of uniaxial anisotropy of Co layers $H_{au1} = H_{au2} \approx 384$ Oe, exchange stiffness of Co $A = 1.6 \cdot 10^{-6}$ erg/cm, saturation magnetization of the Co film $M_S = 1300$ emu/cm^3 [23], gyromagnetic ratio Co $\gamma = 1.9 \cdot 10^7$ Hz/Oe [24]. The wave vector of spin waves was constant $k_x = 11\,\mu$m^{-1}. The field of surface anisotropy of the Co layers $H_{ac1} \approx H_{ac2} \approx 1400$ Oe was determined from the SQUID magnetometry data. From the field dependences of the magnetization recorded when the external field is oriented perpendicular to the sample surface (Fig. 2, curve *1*) and along it (Fig. 2, curve *2*), it follows that in the field $H_{IP} = +8$ kOe the magnetization is $M \approx M_S$. The external magnetic field $H_{IP} = +8$ kOe directed in the sample plane orients the magnetic moments along the field. Thus, the angles between the y axis and the magnetic moments are $\theta_1 = \theta_2 \approx 0°$. Since the samples have perpendicular magnetic anisotropy, the angle between the H_{IP} field and the direction of magnetic anisotropy is $\theta_H = 90°$, and the angles between the y axis and the direction of uniaxial anisotropy of two Co layers are equal to $\theta_{u1} = \theta_{u2} = 90°$. The result of modeling the dependence of the frequency of spin waves on the energy of the interlayer exchange coupling J_{12} is shown in Fig. 4 by solid lines. The solid line *1* in Fig. 4 shows the acoustic mode, and the solid line *2* shows the optical mode. The points in Fig. 4 show the experimental frequencies of the Stokes component of the MBS spectra recorded in a constant field $H_{IP} = +8$ kOe at a constant $k_x = 11\,\mu$m^{-1}. In the absence of interlayer exchange ($J_{12} = 0$), the frequencies of the optical and acoustic modes are close in value [3,25,26]. The triangle in Fig. 4 shows the frequency of the spin wave of the Pt/Co(1.07 nm)/Ir sample [27], which has $J_{12} = 0$, since it contains one ferromagnetic layer. The exchange energy J_{12} between the separated layers of a ferromagnet depends not only on the thickness of the separating layer [9], but also on the thickness of the ferromagnetic layers [28]. In [28] it is shown that the dependence J_{12} on the thickness of one of the ferromagnetic layers can oscillate, i.e. the nature of this dependence is similar to the dependence J_{12} on the thickness of the separating layer [9,28]. This is because the number of atoms decreases in the conducting layer of Co as its thickness decreases, and this ferromagnetic layer becomes less effective as a source of spin-polarized electrons participating in the RKKY interaction. Thus, the value J_{12} in a series of samples under study varies along with the thickness of the upper Co layer. The exchange interlayer energy J_{12} between Co layers in the samples under study was calculated from SQUID magnetometry data. The calculation procedure J_{12} is given in [16]. The thicknesses t_{Co} corresponding to the values J_{12} of the samples are shown on the upper scale of Fig. 4. The frequencies of the peaks in the MBS spectra were determined by their approximation by Lorentz functions using the least squares method. The error in determining the frequencies is used to designate the errors in Figs 4 and 5. The difference in frequency errors for different samples is

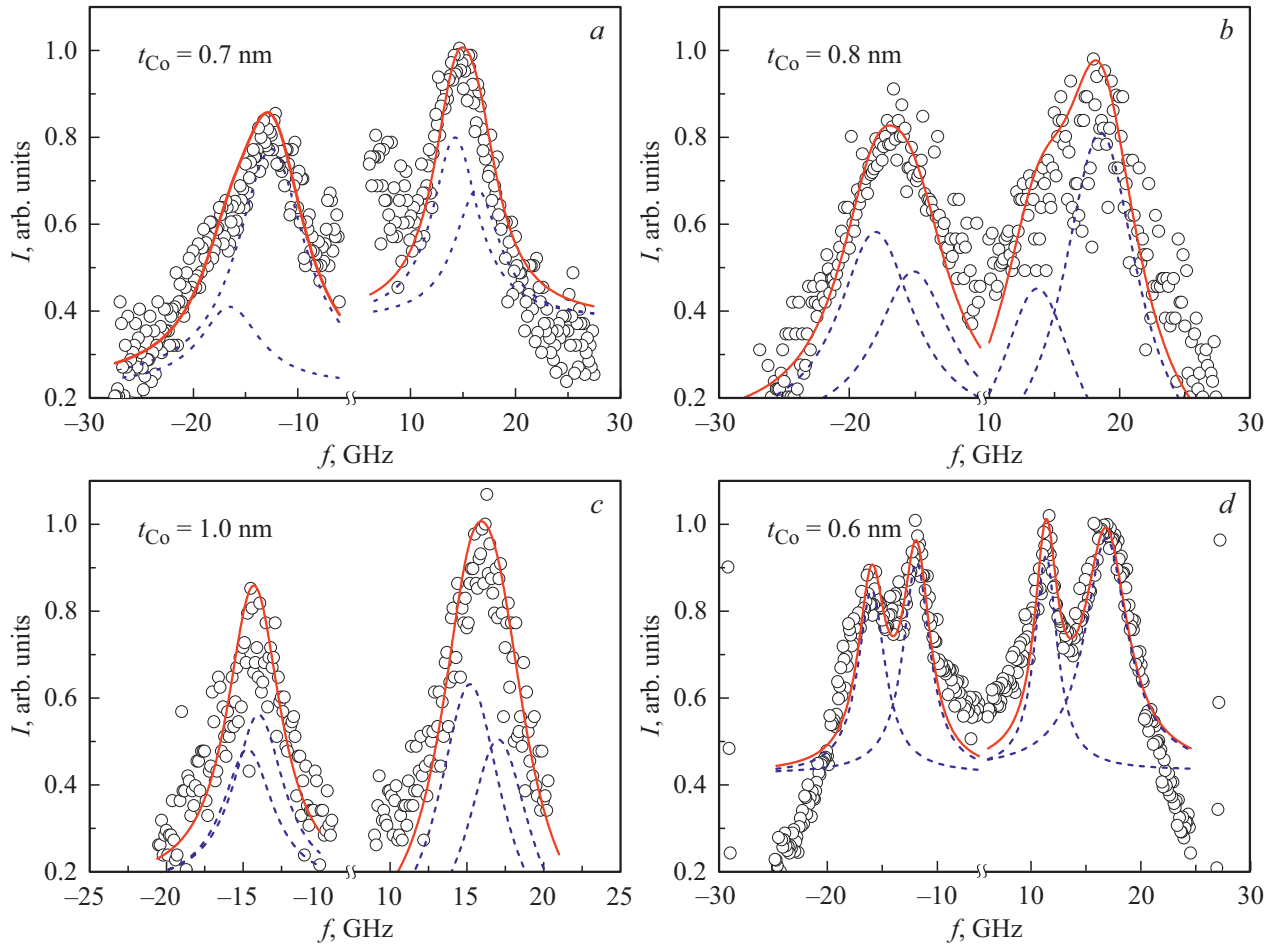

Figure 3. Spectra of Mandelstam-Brillouin spectroscopy recorded in the field $H_{IP} = +8$ kOe at the value of the projection of the wave vector of the laser beam $k_x = 11\,\mu m^{-1}$ for samples with (*a*) $t_{Co} = 0.7$ nm, (*b*) $t_{Co} = 0.8$ nm, (*c*) $t_{Co} = 1.0$ nm, (*d*) $t_{Co} = 0.6$ nm. The dotted lines are the Lorentz components of the decomposition of the experimental spectrum into optical and acoustic modes, described in the text. The solid lines in Fig. 3, *a*–*d* are the sum of the Lorentz lines.

caused by different speed and quality of signal accumulation. The speed and quality of signal accumulation depended not only on the sample, but also on the angle of incidence of the laser beam, and hence on the value of k_x.

The simulation result of the frequency of the optical and acoustic modes coincides with the experimental values of the SW frequencies of the sample with $t_{Co} = 0.6$ nm. The theoretical calculation of the dependence of the optical mode frequency on the interlayer exchange interaction is well compliant with the experimental SW frequencies for samples with $t_{Co} = 0.7$ nm, 0.8 nm, 1.0 nm. For the last three samples, the small difference between the optical and acoustic modes leads to the merging of these two peaks. Since the frequency of the acoustic mode does not depend on J_{12} [2,3], it should be approximately the same for all samples. It is precisely determined for the sample where the peaks of the optical and acoustic branches are separated (~ 16.6 GHz). This made it easier to fit the peaks with two Lorentz functions in those samples with $t_{Co} = 0.7$, 0.8, 1.0 nm, where the acoustic and optical mode peaks merged. The result of spectrum decomposition into two Lorentz peaks is shown in Fig. 3, *a*-*d* by dashed lines. The sum of two Lorentz functions is shown in Fig. 3, *a*–*c* by solid lines. The frequencies of two modes determined by approximation for samples with $t_{Co} = 0.6$, 0.7, 0.8, 1.0 nm are shown in Fig. 4 by points.

In all MBS spectra of the Pt/Co/Ir/Co/Pt samples, a difference was found between the absolute frequencies of the Stokes and anti-Stokes peaks Δf, which is called spin wave nonreciprocity [2]. For acoustic mode peaks, there is no usually frequency nonreciprocity Δf, and the spin wave dispersion plot $f(k_x)$ is a parabola symmetric with respect to $k_x = 0$ (see Fig. 5, *a*). The frequency difference usually occurs for optical modes and can be caused by the difference in the surface anisotropies of the two Co layers [6] and the interface DMI [7]. We assessed the contribution of the difference in the surface anisotropies of the Co layers to the difference in the frequencies of the Stokes and anti-Stokes peaks. The surface anisotropy of the lower Co layers was the same

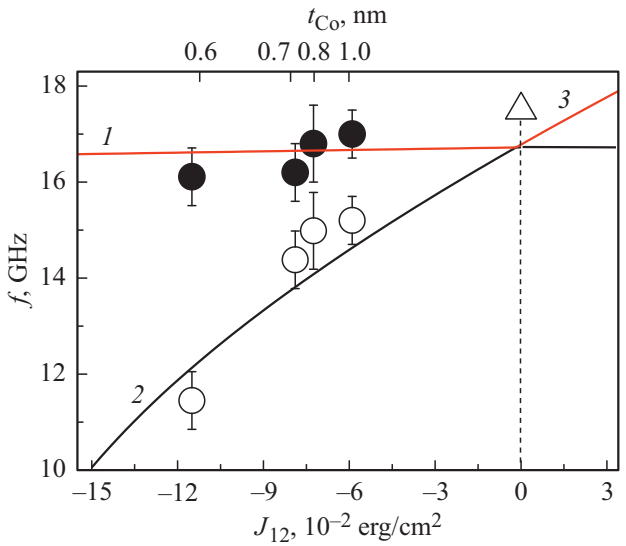

Figure 4. Dependence of the frequency of spin waves on the interlayer exchange energy J_{12} in the field $H_{IP} = +8$ kOe for $k_x = 11\,\mu m^{-1}$. Light symbols show the frequencies of the Stokes peak of the optical mode, and dark symbols show the frequencies of the Stokes peak of the acoustic mode. Point *3* — spin wave frequency ($k_x = 11\,\mu m^{-1}$) for a sample consisting of one Co layer ($J_{12} = 0$) [26]. The solid lines are the theoretical dependences of the frequency of the acoustic mode (line *1*) and the optical mode (line *2*) on the interlayer exchange energy, calculated as part of the model proposed in [14]. The thicknesses of the upper Co layer corresponding to the indicated values J_{12} are given on the upper scale.

for all samples, since they have the same thickness (1.1 nm) and the same Pt (3.2 nm) and Ir (1.4 nm) cover layers. The surface anisotropy constant was calculated from the relation $K_S = K \cdot t_{FM}$, where K is the magnetocrystalline anisotropy constant, t_{FM} is the thickness of the ferromagnetic layer. The magnetocrystalline anisotropy constant is calculated from the relation $K = (H_m \cdot M_S)/2$, where $H_m = H_A + 4\pi M_S$ — field of magnetocrystalline anisotropy, H_A — effective field of magnetic anisotropy. The effective anisotropy field H_A is equal to the field in which the $M(H)$ dependences recorded for two orientations of the magnetic field along the easy magnetization axis and along the hard magnetization axis intersect (Fig. 2). The surface anisotropy constant of the lower layer is $K_{S1} = 0.95$ erg/cm^2. The surface anisotropy constants of the upper Co layers were as follows: for $t_{Co} = 0.6$ nm $K_{S2} = 0.52$ erg/cm^2; for $t_{Co} = 0.7$ nm $K_{S2} = 0.6$ erg/cm^2; for $t_{Co} = 0.8$ nm $K_{S2} = 0.69$ erg/cm^2 and for $t_{Co} = 1.0$ nm $K_{S2} = 0.86$ erg/cm^2. The frequency difference between the MBS peaks, caused by the difference in surface anisotropies, is calculated by the formula [6]:

$$\Delta f = \frac{8\gamma}{\pi^3}\frac{K_{S1} - K_{S2}}{M_S}\frac{k_x}{1 + l_{ex}^2\pi^2/t_{FM}^2}, \qquad (1)$$

where K_{S1} and K_{S2} are the surface anisotropy constants of the pinned and free Co layers, k_x is the projection wave vector of incident light on the x axis, t_{FM} is the thickness of the ferromagnetic layer, $l_{ex} = (2A/4\pi M_S^2)^{1/2}$ is the exchange length. The frequency difference of the MBS peaks calculated from (1) is 0.47–2.27 MHz. This shift is small compared to the experimentally observed frequency difference of $\Delta f\,(k_x) \sim 1$–3 GHz. Thus, the main contribution to the frequency difference is made by the surface DMI.

Formally, the dispersion law for spin waves for a single film [4,7] allows to approximately determine the DMI energy density in a two-layer structure as well

$$2\pi f = \gamma\left(H_{IP} + Jk_x^2 + \xi(k_xL)M_S\right)^{1/2} \times \left(H_{IP} - H_A + Jk_x^2 + M_S - \xi(k_xL)M_S\right)^{1/2} - \frac{2\gamma}{M_S}Dk_x, \qquad (2)$$

where $H_A = 10$ kOe is the effective magnetic anisotropy field determined from SQUID magnetometry data (see Fig. 2), $J = 2A/M_S$ is the exchange constant, L is the ferromagnetic layer thickness, $\xi(k_xL) = 1 - \left(1 - \exp(-|k_xL|)\right)/|k_xL|$. It follows from the dispersion law that D depends on the frequency difference Δf according to the formula

$$D = \frac{\Delta f \pi M_S}{\gamma k_x}. \qquad (3)$$

Equation (3) determined the values D for all four samples of the series (Fig. 6). It can be seen from Fig. 6 that with an increase in the thickness of the upper Co layer, the value D decreases, as in the case of a single Co film [14,29–31]. It is known from the literature that $D \sim 1/t_{Co}$ is inversely proportional to an increase in the thickness t_{Co} of one of the Co layers. The solid line in Fig. 6 shows the approximation of the experimental data by a hyperbola.

For samples based on a single layer of Co [11–14] and for samples based on multiple non-exchanged Co layers of the same thickness, the value D is expected to be the same. The values D of the studied synthetic ferrimagnets (1.7–2.4 erg/cm^2) are greater than the values D for single Co layers, which are shown in Fig. 6 by points *1* and *2* and are equal to 1.4 erg/cm^2. The increase in D compared to a single layer sample can be caused by several factors: 1) an increase in the number of Pt/Co and Ir/Co interfaces on which DMI occurs, 2) decrease in interface roughness; 3) interlayer exchange interaction, which makes DMI in two Co layers not independent of each other, but increases it as a result of spin polarization transfer between the layers.

If the interlayer exchange interaction cannot be neglected, a more complex spin wave dispersion law $f\,(k_x)$ [4] should be used, which takes into account the magnitude and sign of the exchange interaction of two antiferromagnetically coupled layers. The model from [20] was used to describe the dispersion law for spin waves of a synthetic ferrimagnet. It does not take into account the frequency difference Δf caused by DMI, but it takes into account

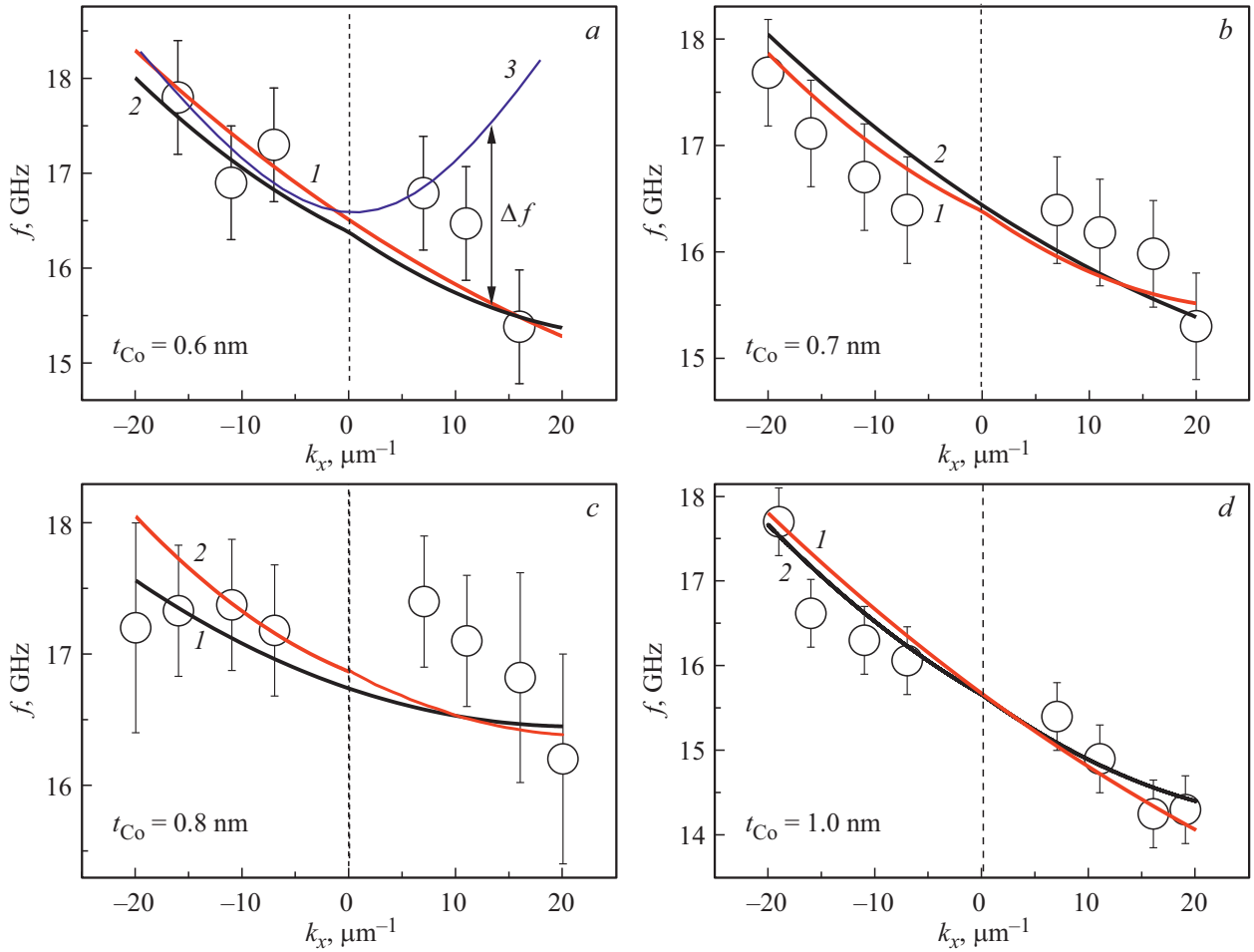

Figure 5. Dependences of the frequency of spin waves f, recorded in a constant magnetic field $H_{IP} = +8$ kOe, on the projection of the laser wave vector k_x onto the x axis for samples with (*a*) $t_{Co} = 0.6$ nm, (*b*) $t_{Co} = 0.7$ nm, (*c*) $t_{Co} = 0.8$ nm, (*d*) $t_{Co} = 1.0$ nm. Solid line *1* — model approximation [14], solid line *2* — equation approximation (2). The solid line *3* in Fig. 5, *a* is the variance of $f(k_x)$ in the lack of DMI.

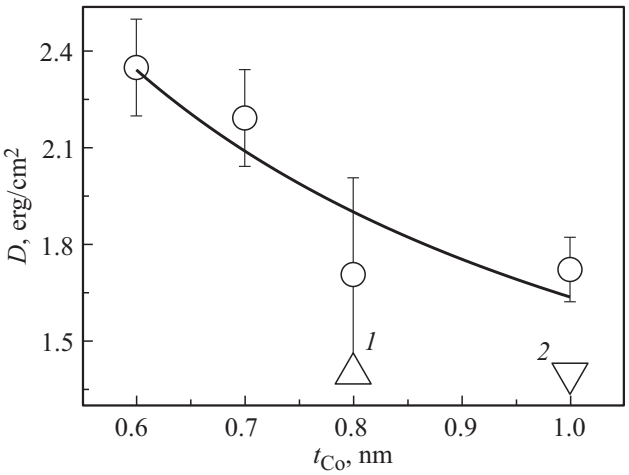

Figure 6. Dependence of the energy density of the interface DMI on the thickness of the upper Co layer t_{Co} in synthetic ferrimagnets Pt(3.2 nm)/Co(1.1 nm)/Ir(1.4 nm)/Co(t_{Co})/Pt(3.2 nm). Point *1* — value D for the Pt/Co(0.8 nm)/Ir heterostructure [20], *2* — value D for the Pt/Co(1.0 nm)/Ir heterostructure [29]. Solid line shows the approximation by hyperbola.

the interlayer exchange interaction between the Co layers. To approximate the dispersion of spin waves with a model from [20], we added to the solution of the equation $f(k_x)$ the difference in the frequencies of the Stokes and anti-Stokes peaks caused by DMI $\Delta f = \gamma D k_x/\pi M_S$, just as it was done for a single-layer sample in formula (3). The result of approximation by modified formulas [20] is shown in Fig. 5, *a*–*d* by solid lines *1*. We used the spin wave dispersion law (2) for comparison, which does not take into account the antiferromagnetic exchange interaction between the Co layers. It is shown in Fig. 5, *a*–*d* by solid lines *2*. Both laws used describe the experimental data satisfactorily. The strong discrepancy between the experimental data and approximations for the sample with $t_{Co} = 0.8$ nm is caused by the measurement error. Thus, the spin wave dispersion law described in [4] can be used to approximate the $f(k_x)$ dependences of synthetic antiferromagnets and ferrimagnets and allows to assess the value of the Dzyaloshinskii–Moriya interaction in them.

4. Conclusion

Acoustic and optical modes of spin waves have been discovered in synthetic ferrimagnets with perpendicular magnetic anisotropy. The contribution of surface anisotropy and DMI to the difference between the frequencies of the Stokes and anti-Stokes peaks of the optical mode was assessed. The main contribution to the frequency difference is made by the interface DMI. As the thickness of the upper Co layer of the Pt/Co/Ir/Co/Pt synthetic ferrimagnet increases, its energy density DMI decreases linearly, as in heterostructures with a single Co layer. The measured values of the energy density DMI D of two exchange-coupled Co layers are greater than the values D of single Co layers. This can be caused by an increase in the number of interfaces at which DMI occurs, by the roughness of the interfaces, and by the presence of an exchange interlayer interaction, due to which individual Co layers contribute to the total DMI. The spin wave dispersion law for single ferromagnetic films qualitatively and quantitatively describes the dispersion in heterostructures consisting of two Co layers coupled by an antiferromagnetic exchange interaction.

Funding

The work was carried out as part of the state assignment AAAA-A19-119092390079-8 of the Institute of Problems of Chemical Physics of RAS. R.B. Morgunov was supported by the grant of the President of the Russian Federation for leading scientific schools 2644.2020.2. A.I. Bezverkhniy was supported by the grant from the Russian Foundation for Basic Research as part of the scientific project No. 19-32-90128. A.V. Sadovnikov and V.A Gubanov were supported by the grant from the Russian Foundation for Basic Research as part of the scientific project No. 18-29-27026.

Conflict of interest

The authors declare that they have no conflict of interest.

References

[1] A. Fert, F. Nguyen Van Dau. Physique **20**, 817 (2019).
[2] P. Grünberg, R. Schreiber, Y. Pang. Phys. Rev. Lett. **57**, 2442 (1986).
[3] J. Barnas, P. Grünberg. J. Magn. Magn. Mater **82**, 186 (1986).
[4] K. Di, V.L. Zhang, H.S. Lim, S. Ch. Ng. Phys. Rev. Lett. **114**, 047201 (2015).
[5] J.J. Krebs, P. Lubitz, A. Chaiken, G.A. Prinz. Phys. Rev. Lett. **63**, 1645 (1989).
[6] S.M. Chérif, Y. Roussigné, P. Moch. J. Appl. Phys. **98**, 063905 (2005).
[7] J. Cho, N.-H. Kim, S. Lee, J.-S. Kim, R. Lavrijsen, A. Solignac, Y. Yin, D.-S. Han, N.J.J. van Hoof, H.J.M. Swagten, B. Koopmans, Ch.-Y. You. Nature Commun. **6**, 7635 (2015).
[8] P.M. Levy, A. Fert. Phys. Rev. B **23**, 4667 (1981).
[9] Y. Roussigné, F. Ganot, C. Dugautier, P. Moch. Phys. Rev. B **52**, 350 (1995).
[10] J. Fassbender, F. Nörtemann, R.L. Stamps, R.E. Camley, B. Hillebrands, G. Güntherodt, S.S.P. Parkin. Phys. Rev. B **46**, 5810 (1992).
[11] S.-G. Je, D.-H. Kim, S.-C. Yoo, B.-C. Min, K.-J. Lee, S.-B. Choe. Phys. Rev. B **88**, 214401 (2013).
[12] R. Lavrijsen, D.M.F. Hartmann, A. van den Brink, Y. Yin, B. Barcones, R.A. Duine, M.A. Verheijen, H.J.M. Swagten, B. Koopmans. Phys. Rev. B **91**, 104414 (2015).
[13] A. Hrabec, N.A. Porter, A. Wells, M.J. Benitez, G. Burnell, S. Mc Vitie, D. Mc Grouther, T.A. Moore, C.H. Marrows. Phys. Rev. B. **90**, 020402(R) (2014).
[14] K. Shahbazi, J.-V. Kim, H.T. Nembach, J.M. Shaw, A. Bischof, M.D. Rossel, V. Jeudy, T.A. More, C.H. Marrows. Phys. Rev. B **99**, 094409 (2019).
[15] N. Nakajima, T. Koide, T. Shidara, H. Miyauchi, H. Fukutani, A. Fujimori, K. Iio, T. Katayama, M. Nývlt, Y. Suzuki. Phys. Rev. Lett. **81**, 5229 (1998).
[16] R. Morgunov, A. Hamadeh, T. Fache, G. Lvova, O. Koplak, A. Talantsev, S. Mangin. Superlat. Microstruct. **104**, 509 (2017).
[17] R.B. Morgunov, A.V. Yurov, V.A. Yurov, A.D. Talantsev, A.I. Bezverhnii, O.V. Koplak. Phys. Rev. B **100**, 144407 (2019).
[18] E.R. Moog, S.D. Bader, J. Zak. App. Phys. Lett. **56**, 2687 (1990).
[19] K. Zakeri. Phys. Rep. **545**, 47 (2014).
[20] S.M. Rezende, C. Chesman, M.A. Lucena, A. Azevedo, F.M. de Aguiar. J. Appl. Phys. **54**, 958 (1998).
[21] B. Hillebrands. Phys. Rev. B **41**, 530 (1990).
[22] A. Haldar, C. Banerjee, P. Laha, A. Barman. J. Appl. Phys. **115**, 133901 (2014).
[23] N. Nozawa, S. Saito, S. Hinata, M. Takahasi. J. Phys. D **46**, 172001 (2013).
[24] M. Belmeguenai, J.-P. Adam, Y. Roussigne, S. Eimer, T. Devolder, J.-V. Kim, S.M. Chérif, A. Stashkevich, A. Thiaville. Phys. Rev. B **91**, 180405(R) (2015).
[25] M. Belmeguenai, H. Bouloussa, Y. Roussigné, M.S. Gabor, T. Petrisor, Jr., C. Tiusan, H. Yang, A. Stashkevich, S.M. Chérif. Phys. Rev. B **96**, 144402 (2017).
[26] N.A. Sergeeva, S.M. Chérif, A.A. Stashkevichm, M.P. Kostylev, J. Ben Yussef. J. Magn. Magn. Mater **288**, 250 (2005).
[27] I.B.-El Mokhtari, D. Ourdani, Y. Roussigné, R.B. Mos, M. Nasui, F. Kail, L. Chahed, S.M. Chérif, A. Stashkevich, M. Gabor, M. Belmeguenai. J. Phys.: Condens. Matter. **32**, 495802 (2020).
[28] L.M. Li, B.-Z. Li, F.-C. Pu. J. Phys.: Condens. Matter **6**, 1941 (2994).
[29] M. Belmeguenai, Y. Roussigné, S.M. Chérif, A. Stashkevich, T. Petrisor jr., M. Nasui, M.S. Gabor. J. Phys. D **52**, 125002 (2019).
[30] N.-H. Kim, J. Jung, J. Cho, D.-S. Han, Y. Yin, J.-S. Kim, H.J.M. Swagten, Ch.-Y. You. Appl. Phys. Lett. **108**, 142406 (2016).
[31] H.T. Nembach, J.M. Shaw, M. Weiler, E.J. Thomas, J. Silvia. Nature Phys. **11**, 825 (2015).